Journal of Alloys and Compounds 509 (2011) 9513–9517

Contents lists available at ScienceDirect

Journal of Alloys and Compounds

journal homepage: www.elsevier.com/locate/jallcom

Annealing driven performance and optical effects in nanocrystalline SnO_2 thin films induced by pulsed delivery

G. He[a,b,*], G. Bhat[b], Z.W. Chen[c,**]

[a] Jiangsu Key Laboratory of Atmospheric Environment Monitoring and Pollution Control, School of Environmental Science and Engineering, Nanjing University of Information Science & Technology, Nanjing 210044, People's Republic of China
[b] Department of Material Science and Engineering (UTNRL), The University of Tennessee, Knoxville, TN 37996, USA
[c] School of Environmental and Chemical Engineering, Shanghai University, Shanghai 200444, People's Republic of China

ARTICLE INFO

Article history:
Received 25 April 2011
Received in revised form 17 July 2011
Accepted 18 July 2011
Available online 26 July 2011

Keywords:
Oxide materials
Thin films
Microstructure
Optical properties

ABSTRACT

Tin dioxide thin films were prepared successfully by pulsed laser deposition techniques on glass substrates. The thin films were then annealed for 30 min from 50 °C to 550 °C at 50 °C intervals. The influence of the annealing temperature on the microstructure and optical properties of SnO_2 thin films was investigated using X-ray diffraction, optical transmittance and reflectance measurements. Various optical parameters, such as optical band gas energy, refractive index and optical conductivity were calculated from the optical transmittance and reflectance data recorded in the wavelength range 300–2500 nm. We found that the SnO_2 thin film annealed at temperatures up to 400 °C is a good window material for solar cell application. Our experimental results indicated that SnO_2 thin films with the high optical quality could be synthesized by pulsed laser deposition techniques.

1. Introduction

Tin dioxide (SnO_2) is a promising wide band gap oxide material because of its higher electronic mobility and wide-band-gap (3.6 eV at 300 K) [1]. It is one of the most important strategic materials and is used for very diverse technological applications such as gas sensing [2], UV sensors [3], electrode materials [4], energy storage and conversion etc. [5,6]. In recent years, the size- and shape-dependent optical and electronic properties of semiconductor nanocrystals have attracted considerable attention. From an application point of view, the use of nanocrystalline particles with a high surface-to-volume ratio made it possible to improve the properties of devices such as gas sensing and optoelectronic devices [7]. Thus, control of size, shape, and microstructure of the nanoparticles are amongst the most important issues in the synthesis of nanomaterials. SnO_2 is widely used under various forms in a broad range of important applications, which have found applications including rechargeable, catalyst supports [8], lithium batteries [9], photovoltaic cells [10].

Being an important *n*-type semiconductor, SnO_2 is transparent in the visible and reflective in the infrared regions. The material possesses high optical transparency in the visible range (up to 80%), low resistivity (10^{-4}–$10^{-6}\ \Omega\,cm^{-1}$), and excellent chemical stability [11]. Recently, SnO_2 thin films have attracted much attention due to their unique microstructures and potential technological applications. It has been showed that SnO_2 thin films as electrodes in organic semiconductors based devices or as electrodes in solar cells covering the front surface of these devices [12]. The immense technological importance keeps SnO_2 thin films under active focus of the research community, and new techniques to modify the properties and behavior are being continually investigated. There are many different techniques used for depositing SnO_2 thin films, for example, electron beam evaporation, reactive thermal evaporation, spray pyrolysis, plasma polymerisation, glow discharge decomposition of tin compounds [13] and other chemical methods [14]. As reported there, all available methods require high substrate temperature or post deposition annealing for the fabrication of good quality polycrystalline films. The influence of annealing temperature on material properties is especially remarkable. High temperature, however, damages the surface of thin films and increases the interface thickness, which has negative effects on optical properties, particularly on waveguide properties.

Pulsed laser deposition (PLD) is a growth technique in which photonic energy is coupled to the bulk starting material via electronic processes [15]. An intense laser pulse passes through an optical window of a vacuum chamber and is focused onto a target. Above a certain power density, significant material removal

* Corresponding author at: Jiangsu Key Laboratory of Atmospheric Environment Monitoring and Pollution Control, School of Environmental Science and Engineering, Nanjing University of Information Science & Technology, Nanjing 210044, People's Republic of China. Tel.: +86 25 5873 1090; fax: +86 25 5873 1089.
** Corresponding author. Tel.: +86 25 5873 1090; fax: +86 25 5873 1089.
E-mail addresses: hegang@jlonline.com (G. He), zwchen@shu.edu.cn (Z.W. Chen).

0925-8388/$ – see front matter © 2011 Elsevier B.V. All rights reserved.
doi:10.1016/j.jallcom.2011.07.053

occurs in the form of an ejected luminous plume. The threshold power density needed to produce such a plume depends on the target material, its morphology, and the laser pulse wavelength and duration, but might be of the order of 10–500 MW/cm^2 for ablation using ultraviolet excimer laser pulses of 10 ns duration. Material from the plume is then allowed to re-condense on a substrate, where thin film growth occurs. The growth process may be supplemented by a passive or reactive gas or ion source, which may affect the ablation plume species in the gas phase or the surface reaction [16]. The diversity of thin films grown using PLD is enormous and it arguably offers more flexibility than anything else. The rationale for using PLD in preference to other deposition techniques lies primarily in its pulsed nature, the possibility of modifying surface chemistry far from thermal equilibrium, and under favorable conditions, the ability to reproduce in thin films the same elemental ratios of even highly chemically complex bulk ablation targets [17]. The physical processes in PLD are highly complex and interrelated, and depend on the laser pulse parameters and the properties of the target material [18]. PLD offers many advantages of reduced contamination due to the use of laser light, control of the composition of deposited structure and in situ doping. It is a versatile and powerful tool for the production of nanoparticles with desired size and composition under appropriate control of the experimental deposition conditions [15]. PLD techniques have been successfully applied for growing quality tin oxide thin films. They were produced by ablation of either a Sn target in an oxidizing oxygen atmosphere or a SnO_2 target [19].

In order to provide guidance for the search of better sensor materials with suitable optical properties, it is necessary to investigate the temperature effects of the semiconductor oxide gas sensors. In this paper, the microstructural properties of SnO_2 thin films deposited on glass substrates by pulsed laser deposition techniques were investigated before and after thermal annealing in the temperature range from 50 °C to 550 °C at 50 °C intervals. X-ray diffraction results confirmed that the various SnO_2 thin films consisted of nanoparticles with average grain size in the range of 23.7–28.9 nm. An interesting effect can be achieved by shining UV light onto SnO_2 to create electron and hole carriers, which allows switching between states of high (UV on) and low (UV off) conductivity [20]. The transmittance measurements indicated that present SnO_2 thin films can be used as a window material for solar cell application due to their best transmittance of films is around 85%. Various optical parameters such as optical band gas energy, refractive index and optical conductivity were calculated from the optical transmittance and reflectance data recorded in the wavelength range 300–2500 nm. It is well established that in ordinary semiconductors electron–electron interactions are essential to explain their optical properties. We found that the optical band gas energy and refractive index of SnO_2 thin films annealed at various temperatures presented approximately linear behavior, and SnO_2 thin films exhibited high optical conductivity. These findings revealed that present SnO_2 thin films annealed up to 400 °C are a good window material for solar cell application.

2. Experimental details

The as-grown SnO_2 thin films were synthesized by the laser ablation method reported elsewhere [8]. The target for pulsed laser deposition (PLD) was a sintered SnO_2 disc. The method employed to synthesize the pure SnO_2 powder is described by the direct oxidation reaction at 1050 °C, viz.: $Sn + O_2 \rightarrow SnO_2$, carried out in a horizontal quartz tube. The circular target consisted of high-purity cassiterite SnO_2 (99.8%). The size of the target was about ϕ15 mm × 4 mm, and it was cleaned with methanol in an ultrasonic cleaner before installation to minimize contamination. The laser used was a KrF excimer laser (Lambda Physik, LEXtra 200, Germany) producing pulse energies of about 350 mJ at a wavelength of 248 nm and a frequency of 10 Hz. The duration of every excimer laser pulse was 34 ns. The laser energy was transmitted onto the target in a high-vacuum chamber through an ultraviolet (UV)-grade fused silica window using an UV-grade fused silica lens. During the experiment, the target was rotating at a rate of 15 rpm to avoid drilling. The fluence was set at 5 J/cm^2 per pulse, corresponding to a total of approximately 1.5×10^5 laser pulses. The growth rate was estimated to be about 3×10^{-1} nm/s (or about 1 μm/h). The ablated substance was collected on a clean glass substrate, which was mounted on a substrate holder 2.5 cm away from the target. The high vacuum in the deposition chamber was achieved by using a cryopump (Edwards Coolstar 800). The base pressure prior to laser ablation was about 1×10^{-6} mbar, and the working pressure during laser ablation was about 2×10^{-6} mbar.

The as-prepared thin films were annealed at various temperatures ranging from 50 °C to 550 °C at 50 °C intervals for a fixed time of 30 min at each temperature. Structure of these thin films was determined by recording X-ray diffraction (XRD) patterns at room temperature using a Philips X'pert diffractometer equipped with Cu K_α radiation (1.5406 Å) in reflection geometry. Proportional counter with an operating voltage of 40 kV and a current of 40 mA was used. XRD patterns were recorded at a scanning rate of 0.05 s^{-1} in the 2θ ranges from 20° to 60°. Optical transmittance and reflectance of as-prepared and annealed thin films were recorded at room temperature by a DUU-3700 spectrophotometer in the wavelength range 300–2500 nm.

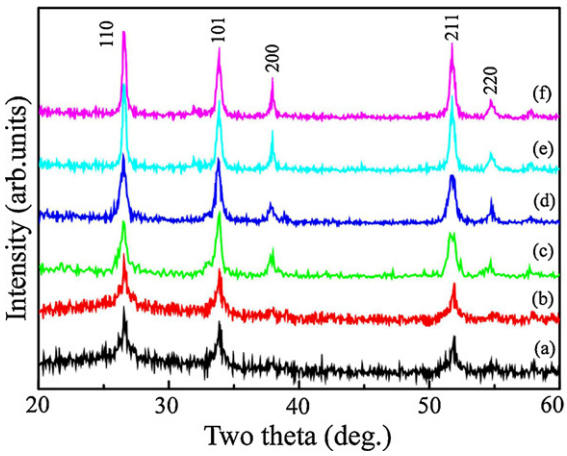

Fig. 1. XRD patterns of SnO_2 thin films annealed at different temperatures for 30 min. (a) As-prepared thin film; (b) 100 °C; (c) 200 °C; (d) 300 °C; (e) 400 °C; and (f) 500 °C.

3. Results and discussion

SnO_2 has a tetragonal rutile crystalline structure (known in its mineral form as cassiterite) with point group D_{4h}^{14} and space group $P4_2/mnm$. The unit cell consists of two metal atoms and four oxygen atoms. Each metal atom is situated amidst six oxygen atoms which approximately form the corners of a regular octahedron. Oxygen atoms are surrounded by three tin atoms which approximate the corners of an equilateral triangle. The lattice parameters are $a = b = 4.7382(4)$ Å, and $c = 3.1871(1)$ Å [21]. The study of microstructural properties of SnO_2 thin films is significant for the understanding of whole structural features and the fabrication of novel functional materials with favorable properties. Fig. 1 shows the XRD patterns of SnO_2 thin films annealed at different temperatures for 30 min. The XRD patterns show that the thin film deposited at room temperature is predominantly amorphous as indicated by the broad diffraction peaks shown in Fig. 1a. When the annealing temperature reaches 100 °C, the amount of the amorphous phase is reduced. With further increase of the annealing temperature, the thin films become more crystalline as manifested by the sharper peaks. It can be seen that all the thin films are polycrystalline with the SnO_2 tetragonal structure shown in Fig. 1b. No characteristic peak such as tin oxide crystals or impurities is detected. The ($h\,k\,l$) peaks observed are (1 1 0), (1 0 1), (2 0 0), (2 1 1), and (2 2 0). The high intensity of these peaks suggests that these thin films mainly consist of the crystalline phase. As the annealing temperature is increased, the crystallinity of the thin films is enhanced as manifested by the intensity and sharpness of the XRD peaks of the SnO_2 thin films annealed at 200, 300, 400, and 500 °C

shown in Fig. 1c–f, respectively. The temperature dependence can be interpreted mainly by the mobility of the atoms in thin films at different temperatures. At low temperature, the vapor species have a low surface mobility and will be located at different positions on the surface. The low mobility of the species will prevent full crystallization of the thin films. However at high temperatures species with high enough mobility will arrange themselves at suitable positions in the crystalline cell [22–24]. The SnO_2 average grain sizes were calculated using the Scherrer formula:

$$D = \frac{K\lambda}{\beta \cos\theta}, \quad (1)$$

where D is the diameter of the nanoparticles, $K = 0.9$, $\lambda(\mathrm{Cu}\,K_\alpha) = 1.5406$ Å, and β is the full-width-at-half-maximum of the diffraction lines. The results show that the average grain sizes of the as-prepared and the annealed SnO_2 nanoparticles are in the range of 23.7–28.9 nm. SnO_2 nanoparticle size decreases from 27.6 nm (at room temperature) to smaller than 23.7 nm at 200 °C. It then sharply increases to 27.1 nm at 300 °C, followed by a gradual decrease to 25.7 nm at 400 °C. It finally increases to 28.9 nm upon further annealing at higher temperatures. In fact, metal oxide nanostructures can work as sensitive and selective chemical sensors. Nanostructured sensor elements can be configured as resistors whose conductance can be modulated by charge transfer across the surface or as a barrier junction device whose properties can be controlled by applying potential across the junction. Functionalizing the surface further offers a possibility to improve their sensing ability.

The information of optical transmittance is important in evaluating the optical performance of semiconducting oxide thin films. Fig. 2 shows the optical transmittance spectra for (a) the as-prepared thin film, and those annealed for 30 min at the following temperatures: (b) 100 °C, (c) 200 °C, (d) 300 °C, (e) 400 °C, and (f) 500 °C. It can be seen that the transmittance behavior of all thin films was similar in the wavelength range 300–2500 nm. The values of transmittance for the as-prepared thin film and the thin films annealed up to 400 °C are larger (>75.3%) than that for the thin film annealed at 500 °C (<48.7%) in the wavelength range 300–750 nm. It was also found that the best transmittance of films is around 85%. However, here are two strong peaks in this figure which is different from other reports, one is near by 530 nm the other in the vicinity of 730 nm. This wavelength range almost covers the entire solar spectrum. Tin oxide film presents high transmittance in visible region being suitable for several applications where one needs good transparency and conductivity. So the observation confirm that these SnO_2 films expect annealed 500 °C are highly transparent oxide relatively to the common solar spectra. Thus, the thin films annealed up to 400 °C can be adopted as a window material for solar cell devices due to its high transmittance. The large and slow decrease of transmittance in the infrared (IR) region can be attributed to free carrier absorption. Similarly optical characterization also was found by Bhatti and co-authors in their SnO_2 thin films by using different method: rf-magnetron sputtered technique [25]. Our experimental results indicated that SnO_2 thin films with the high optical quality could be synthesized by PLD techniques. If there is absorption or scattering then by conservation of energy we must have that [26]

$$A + R + T = 1, \quad (2)$$

$$A \approx \alpha L, \quad (3)$$

Fig. 3 shows the optical reflectance spectra of (a) the as-prepared SnO_2 thin film and those annealed for 30 min at the following temperatures: (b) 100 °C, (c) 200 °C, (d) 300 °C, (e) 400 °C, and (f) 500 °C. The reflectance of the as-prepared and annealed thin films shows very similar behavior in the entire wavelength range. When the

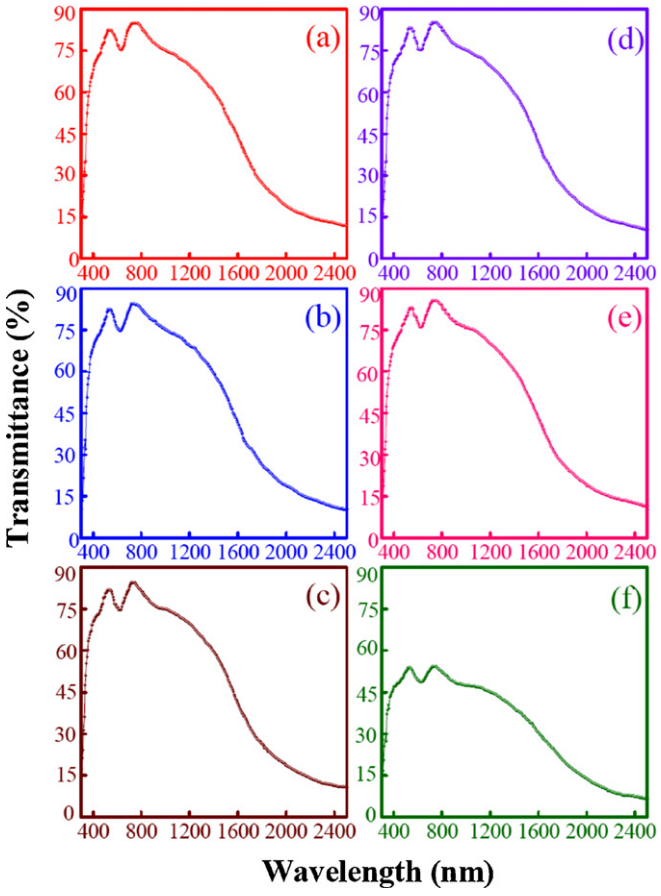

Fig. 2. Optical transmittance spectra of SnO_2 thin films annealed at different temperatures for 30 min. (a) As-prepared thin film; (b) 100 °C; (c) 200 °C; (d) 300 °C; (e) 400 °C; and (f) 500 °C.

thin film was annealed at 500 °C, the transmittance of the thin film decreased. We speculate that any variation in transmittance and reflectance caused by the annealing process might be related to the rearrangement of atoms and/or grain growth, etc. to remove residual stresses/defects formed during thin film deposition [25].

A solar cell is basically a semiconductor diode. It is known that semiconductor material absorbs the incoming photons and converts them into electron–hole pairs. The determinative parameter is the band-gap energy E_g of the semiconductor in this photogeneration step [27]. To calculate the band gap energy (E_g) of all the thin films, the following relation was applied

$$(\alpha h\nu)^2 = B^2(h\nu - E_g) \quad (4)$$

in which the absorption coefficient α was determined from the transmittance data using the formula

$$T = e^{-\alpha L}. \quad (5)$$

If the absorption coefficient at shorter wavelengths was determined from this relation

$$\alpha = \frac{2.303}{L} lg \frac{1-R}{T}, \quad (6)$$

where B is a constant, T is the transmittance, R is the reflectance and L is thickness of the thin films. The graphs of $(\alpha h\nu)^2$ versus photon energy ($h\nu$) are drawn for the as-prepared and annealed thin films. The values of E_g obtained from the extrapolation of the linear portion of these curves to $(\alpha h\nu)^2 = 0$ are plotted in Fig. 4a as a function of annealing temperature. Fig. 4a shows a decrease in band gap energy as the annealing temperature is increased. The annealing may lead

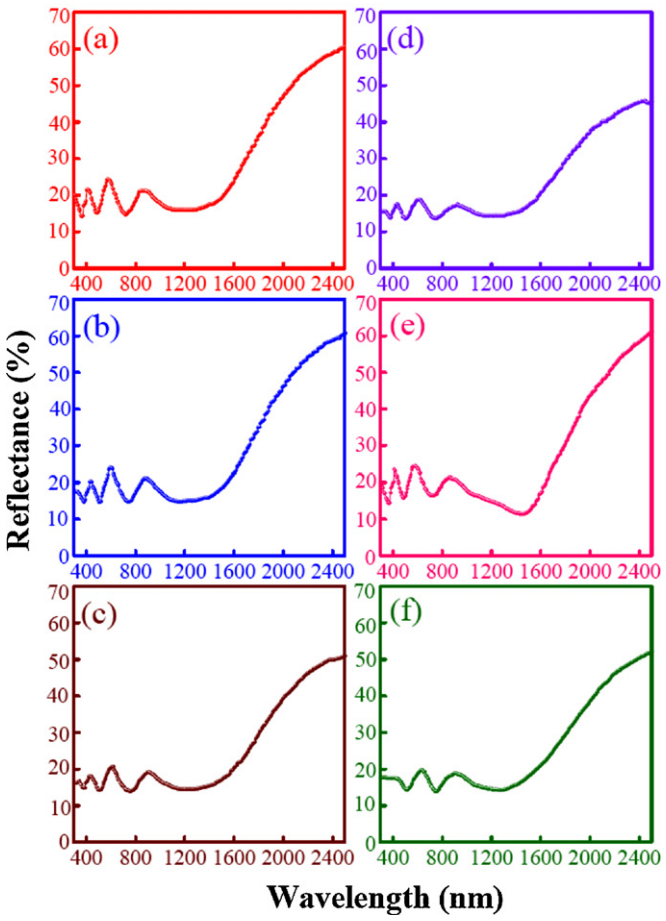

Fig. 3. Optical reflectance spectra of SnO_2 thin films annealed at different temperatures for 30 min. (a) As-prepared thin film; (b) 100 °C; (c) 200 °C; (d) 300 °C; (e) 400 °C; and (f) 500 °C.

to a direct renormalization of band gap energy due to the temperature dependence of electron phonon interactions [28]. While the effect is embodied in the famous Elliott's formula [29] that describes the intensity of optical absorption close to the gap edge. So the approach to quantitative determination of the size dependence of the band gap energy is based on the effective mass approximation. The increase in optical band gap (ΔE_g) of a nanocrystalline semiconductor may be represented as

$$\Delta E_g = E_g^{nano} - E_g^{bulk} = \frac{h^2}{8\mu R^2} - \frac{1.8e^2}{\varepsilon R}, \quad (7)$$

where E_g^{nano} is the band gap energy of the nanocrystalline material, E_g^{bulk} is the band gap energy of the material in bulk form, μ is the electron-hole effective mass, and ε is the static dielectric constant. The first term in this formula represents the particle-in-a-box quantum localization energy and has simple R^{-2} dependence, where R is the particle radius. The second term represents the Coulomb energy with R^{-1} dependence. The radii of the SnO_2 nanocrystals calculated from this formula match reasonably well with the previously calculated values [30]. Therefore, it can be assumed that during the annealing process atoms can rearrange themselves into more energetic and suitable positions in the valence band and cause the mean free path of electrons to increase, thus less energy is required by an electron to jump from the valence to the conduction band. Fig. 4b is a graph of refractive index (n) versus annealing temperature of SnO_2 thin films at wavelength $\lambda = 589.3$ nm, which indicates a decreasing trend with increasing annealing temperature. The refractive index values measured at $\lambda = 589.3$ nm are in

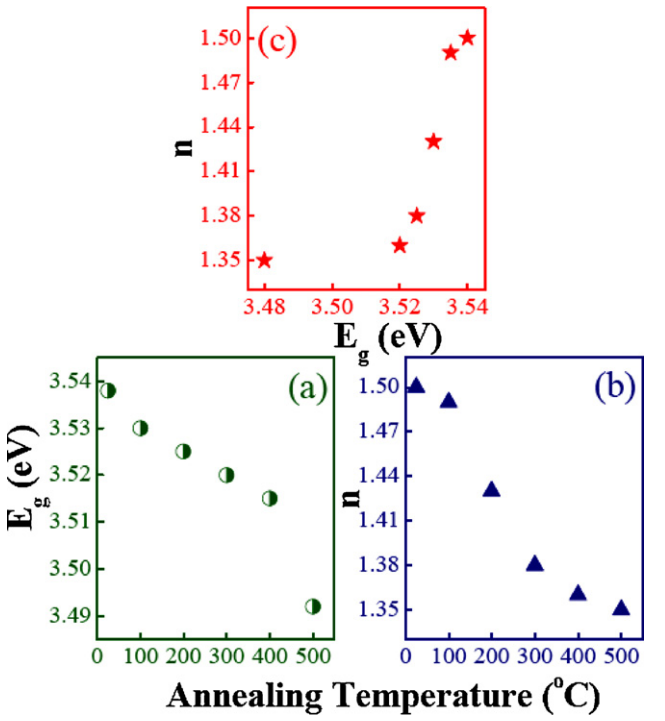

Fig. 4. (a) Graph of optical band gap (E_g) versus annealing temperature for SnO_2 thin films. (b) Graph of refractive index (n) versus annealing temperature for SnO_2 thin films at wavelength $\lambda = 589.3$ nm. (c) Graph of optical band gap (E_g) against refractive index (n) for SnO_2 thin films.

the range 1.49–1.36. In order to establish a relationship between the refractive index (n) and the optical band energy (E_g), a graph was plotted as shown in Fig. 4c. An approximately linear relationship is found with

$$n = 2.1667E_g - 6.1801. \quad (8)$$

Fig. 5 shows the graph of optical conductivity (σ) versus wavelength for SnO_2 thin films annealed at different temperatures for 30 min: (a) the as-prepared thin film, (b) 100 °C, (c) 200 °C, (d) 300 °C, (e) 400 °C, and (f) 500 °C. It is also can predicts that the optical conductivity of SnO_2 films has the form:

$$\sigma(\omega) = \sigma_o\theta(\hbar\omega - 2\mu), \quad (9)$$

where

$$\sigma_o = \frac{\pi e^2}{2h}, \quad (10)$$

$\hbar\omega$ is the photon energy and $\theta(x)$ is the Heaviside step function [31]. This figure shows a rapid rise of optical conductivity (σ) in the IR region. The result can be explained by an enhancement of crystallinity, and an increase of the grain size with annealing temperature. The value of optical conductivity (σ) was found to be very high, which may be applied to photovoltaic cells. An interesting found that SnO_2 thin film at annealing temperature 500 °C has a better optical conductivity than other conditions. The optical conductivity of film annealed at 100 °C is slightly higher than annealed at 200 °C, 300 °C, and 400 °C in the far-infrared region. To sum up, from the present investigation it can be concluded that the SnO_2 thin films annealed up to 400 °C can be used as a good window material for solar cell application due to their best transmittance of films is around 85% and 400 °C may be the optimum annealing temperature. The optical band gap energy and refractive index of the present thin films annealed at various temperatures show approximately linear behavior, and the SnO_2 thin films display high optical conductivity. These findings indicate that these SnO_2 thin

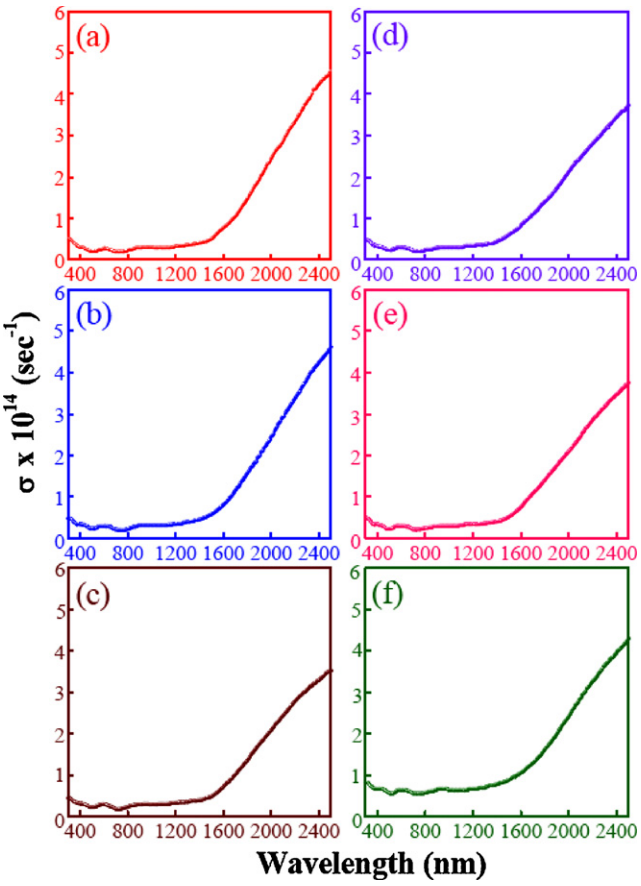

Fig. 5. Graph of optical conductivity (σ) versus wavelength of SnO_2 thin films annealed at different temperatures for 30 min. (a) As-prepared thin film; (b) 100 °C; (c) 200 °C; (d) 300 °C; (e) 400 °C; and (f) 500 °C.

films have potential technological applications in the fabrication of solar cell devices and gas sensors.

4. Conclusions

In summary, the microstructural and optical properties of SnO_2 thin films deposited on glass substrates by PLD techniques were investigated before and after thermal annealing in the temperature range from 50 °C to 550 °C at 50 °C intervals. X-ray diffraction results confirmed that the various SnO_2 thin films consisted of nanoparticles with average grain size in the range of 23.7–28.9 nm. The microstructural analysis of the SnO_2 gas-sensing materials demonstrated that the annealing temperature is a very important parameter. It affects crystalline microstructure and optical properties of the thin films. The transmittance measurements indicated that present SnO_2 thin films can be used as a window material for solar cell devices due to their best transmittance of films is around 85%. Various optical parameters such as optical band gas energy, refractive index and optical conductivity were calculated from the optical transmittance and reflectance data recorded in the wavelength range 300–2500 nm. We found that the optical band gas energy and refractive index of SnO_2 thin films annealed at various temperatures presented approximately linear behavior, and SnO_2 thin films exhibited high optical conductivity. These findings revealed that SnO_2 thin film annealed up to 400 °C is a good window material for solar cell devices. This point will be studied in the immediate future. Our experimental results indicated that SnO_2 thin films with the high optical quality could be synthesized by PLD techniques.

Acknowledgements

The work described in this article was financially supported by the Nanjing University of Information Science & Technology Foundation (20080314), Shanghai Committee of Science and Technology (10JC1405400), and Shanghai Leading Academic Discipline Project (S30109).

References

[1] S. Gubbala, V. Chakrapani, V. Kumar, M.K. Sunkara, Adv. Funct. Mater. 18 (2008) 2411–2418.
[2] M. Law, H. Kind, B. Messer, F. Kim, P.D. Yang, Angew. Chem. Int. Ed. 41 (2002) 2405–2408.
[3] Z. Liu, D. Zhang, S. Han, C. Li, T. Tang, W. Jin, X. Liu, B. Lei, C. Zhou, Adv. Mater. 15 (2003) 1754–1757.
[4] C. Kim, M. Noh, M. Choi, J. Cho, B. Park, Chem. Mater. 17 (2005) 3297–3301.
[5] C. Nayral, E. Viala, P. Fau, F. Senocq, J.C. Jumas, A. Maisonnat, B. Chaudret, Chem. Eur. J. 6 (2000) 4082–4090.
[6] S. de Monredon, A. Cellot, F. Ribot, C. Sanchez, L. Armelao, L. Gueneau, L. Delattre, J. Mater. Chem. 12 (2002) 2396–2400.
[7] F. Gu, S. Wang, H. Cao, C. Li, Nanotechnology 19 (2008) 095708.
[8] Y.A. Cao, X.T. Zhang, W.S. Yang, H. Du, Y.B. Bai, T.J. Li, J.N. Yao, Chem. Mater. 12 (2000) 3445–3448.
[9] P. Meduri, C. Pendyala, V. Kumar, G.U. Sumanasekera, M.K. Sunkara, Nano Lett. 9 (2009) 612–616.
[10] H. Huang, O.K. Tan, Y.C. Lee, T.D. Tran, M.S. Tse, X. Yao, Appl. Phys. Lett. 87 (2005) 163123.
[11] Q. Kuang, C. Lao, Z.L. Wang, Z. Xie, L.S. Zheng, J. Am. Chem. Soc. 129 (2007) 6070–6071.
[12] L. Roman, R. Valaski, C.D. Canestraro, Appl. Surf. Sci. 252 (2006) 5361–5364.
[13] Z.W. Chen, J.K.L. Lai, C.H. Chek, H.D. Chen, Appl. Phys. A: Mater. Sci. Process. 81 (2005) 1073–1076.
[14] J.H. Sung, Y.S. Lee, J.W. Lim, Y.H. Hong, D.D. Lee, Sens. Actuators B 66 (2000) 149–152.
[15] D.B. Chrisey, G.K. Hubler, Pulsed Laser Deposition of Thin Films, Wiley, New York, 1994.
[16] O. Auciello, J. Engemann, Multicomponent and Multilayered Thin Films for Advanced Microtechnologies: Techniques Fundamentals and Devices, Kluwer, Netherlands, 1993.
[17] D. Bäuerle, Laser Processing and Chemistry, Springer, New York, 1996.
[18] M. von Allmen, A. Blatter, Laser-Beam Interactions with Materials, Springer, New York, 1995.
[19] R. Dolbec, M.A. El Khakani, A.M. Serventi, R.G. Saint-Jacques, Sens. Actuators B 93 (2003) 566–571.
[20] S. Mathur, S. Barth, H. Shen, J. Pyun, U. Werne, Small 1 (2005) 713–717.
[21] G. McCarthy, J. Welton, J. Powder Diffract. 4 (1989) 156.
[22] H.R. Fallah, M. Ghasemi, A. Hassanzadeh, Physics E 39 (2007) 69–74.
[23] Z.W. Chen, C.M.L. Wu, C.H. Shek, J.K.L. Lai, Z. Jiao, M.H. Wu, Crit. Rev. Solid State Mater. Sci. 33 (2008) 197–209.
[24] Y.J. Kim, Y.T. Kim, H.K. Yang, J.C. Park, J.I. Han, Y.E. Lee, H.J. Kim, J. Vac. Sci. Technol. A 15 (1997) 1103.
[25] M.T. Bhatti, A.M. Rana, A.F. Khan, Mater. Chem. Phys. 84 (2004) 126–130.
[26] M. Fox, Optical Properties of Solids, Oxford University, Oxford, 2001.
[27] A. Shah, P. Torres, R. Tscharner, N. Wyrsch, H. Keppner, Science 285 (1999) 692–698.
[28] D. Olguín, M. Cardona, A. Cantarero, Solid State Commun. 122 (2002) 575–589.
[29] H. Haug, S.W. Koch, Phys. Rev. A 39 (1989) 1887–1898.
[30] S. Das, S. Kar, S. Chaudhuri, J. Appl. Phys. 99 (2006) 114303.
[31] N.M.R. Peres, R.M. Ribeiro, A.H. Castro Neto, Phys. Rev. Lett. 105 (2010) 055501.